

Ferromagnetic filament shapes in a rotating field reveal their magnetoelastic properties

A. P. Stikuts^{*1}, A. Cēbers^{†1}, and G. Kitenbergs^{‡1}

¹MMML lab, Department of Physics, University of Latvia,
Jelgavas 3, Riga, LV-1004, Latvia

June 2023

Abstract

Flexible ferromagnetic filaments can be used to control the flow on the micro-scale with external magnetic field. To accurately model them, it is crucial to know their parameters such as their magnetization and bending modulus, the latter of which is hard to determine precisely. We present a method how the ferromagnetic filament's shape in a rotating field can be used to determine the magnetoelastic number Cm - the ratio of magnetic to elastic forces. Then once the magnetization of the filament is known, it is possible to determine its bending modulus. The main idea of the method is that Cm is the only parameter that determines whether the filament is straight or whether its tips are bent towards the magnetic field direction. Comparing with numerical solutions, we show that the method results in an error of 15...20% for the determined Cm , what is more precise than estimations from other methods. This method will allow to improve the comparability between theoretical filament models and experimental measurements.

1 Introduction

Magnetic filaments can be created by connecting paramagnetic or ferromagnetic beads with a linker, for example, DNA fragments or some other polymer [1, 2, 3, 4]. The resulting filaments are typically tens of microns long. The diameter of the beads (and thus the width of the filament) range from less than a micron for the paramagnetic case [1] to 4 μm for the ferromagnetic case [5]. Apart from the

*andris.pavils.stikuts@lu.lv

†andrejs.cebers@lu.lv

‡guntars.kitenbergs@lu.lv

choice of the beads, another variable that determines the properties of the filaments is the choice and length of the linker polymers. The impact of DNA linker length to the filament’s flexibility was analyzed in ref. [6]. Magnetic filaments can be used to influence the flow on the micro-scale using external magnetic fields. A few of their applications include microswimming [7, 8], micromixing [9, 10], and navigation through microfluidic channels [11].

To describe such filaments theoretically [12], it is vital to accurately determine their magnetization M and bending modulus A_B (such that the associated energy is $A_B \int k^2 dl/2$, where k is the curvature of the filament). The magnetization depending on the applied magnetic field can be determined from bulk measurements of the beads that make up the filaments [5]. The determination of the bending modulus A_B requires more subtle techniques since the filaments are micron-sized. Paramagnetic filaments when placed in a static field form long lived metastable hairpin-like U shapes, whose maximum curvature k_{max} for strong fields is proportional to the square root of the magnetoelastic number Cm (the ratio of magnetic to elastic forces) [12, 13]. From this it is possible to determine the value of A_B [1]. Theoretically stationary U shapes can also be achieved with ferromagnetic filaments, however they are more unstable than the paramagnetic U shapes, and quickly relax to straight shapes through the third dimension. Nonetheless it has been attempted to estimate A_B by observing the curvature just before the relaxation [5]. Another approach uses the fact that a slightly deformed filament exponentially relaxes to a straight shape with the characteristic time $t_0 = \zeta_{\perp} L^4/A_B$, where ζ_{\perp} is the drag coefficient in the direction normal to the filament’s centerline [14]. Using this method, A_B was estimated in ref. [15], where the drag coefficient was estimated $\zeta_{\perp} \approx 4\pi\eta$ with η being the viscosity of the surrounding fluid. This, however, might be an underestimate since the filaments are close to the bottom of the sample cell and the drag close to it rapidly increases [16].

Many experimental works [5, 8, 15, 17, 18] use ferromagnetic filaments formed using streptavidin coated micron sized ($d = 4.26\mu m$) ferromagnetic beads (Spherotec, 1%w/v) that are linked with 1000bp long biotinized DNA fragments (ASLA biotech or Latvian Biomedical Research and Study Centre) following the procedure outlined in [19]. The estimated bending modulus A_B values for some of these works are gathered in table 1. There is a variation of several orders of magnitude, which motivates us to devise a relatively simple procedure to determine the filament’s bending modulus.

Method	$A_B, J \cdot m$
U shape curvature estimation [5]	$1.5 \cdot 10^{-19}$
Relaxation to a straight shape ¹ [15]	$4.1 \cdot 10^{-23}$
Fitting of numerical 3D precessing shape [18]	$1.5 \cdot 10^{-21}$

Table 1: The determined bending modulus A_B of several experimental works that use the same type of ferromagnetic filaments.

In this work we show how a ferromagnetic filament's shape in a rotating field can be used to determine the magnetoelastic number Cm and thus the bending modulus A_B . We solve for the equilibrium shape of the filament for small deviation from the magnetic field direction. We then extend this solution to include large deviations when Cm is small. Finally we outline the procedure how to determine the filament's parameters and compare it to full numerical simulations to determine its accuracy.

2 Mathematical model

Elastic magnetic filaments are commonly modeled using Kirchhoff theory of an elastic rod with additional terms that describe the magnetic interactions [12, 20]. The filament of length L is described by the radius vector $\mathbf{r}(l)$ which is parameterized by the arc length $l \in [-L/2, L/2]$. The force acting on the cross-section of the filament reads

$$\mathbf{F} = -A_B \mathbf{r}_{lll} + \Lambda \mathbf{r}_l + \mathbf{F}_m, \quad (1)$$

where the subscript l denotes the derivative with respect to the arc length, A_B is the bending modulus and $\Lambda(l)\mathbf{r}_l$ is the tension force that ensures the inextensibility of the filament. \mathbf{F}_m is the magnetic force that for a ferromagnetic filament reads

$$\mathbf{F}_m = -\mu_0 M \mathbf{H}, \quad (2)$$

where M is the magnetic moment per unit length of the filament, and \mathbf{H} is the applied magnetic field intensity.

When the filament is slender, its motion can be described by the resistive-force theory [21]. The linear force density in a Stokes flow is connected with the velocity through the drag coefficients parallel to the filament ζ_{\parallel} and perpendicular to it ζ_{\perp}

$$\mathbf{F}_l = \zeta_{\perp}((\mathbf{v} - \mathbf{v}_{\infty}) \cdot \mathbf{n})\mathbf{n} + \zeta_{\parallel}((\mathbf{v} - \mathbf{v}_{\infty}) \cdot \mathbf{t})\mathbf{t}, \quad (3)$$

where \mathbf{t} and \mathbf{n} is the tangent and normal vectors of the filament, respectively, and \mathbf{v}_{∞} is the background flow velocity. The local inextensibility of the filament dictates that

$$\mathbf{r}_l \cdot \mathbf{r}_l = 1. \quad (4)$$

Taking the time derivative of equation (4) we get a constraint on the velocity $\mathbf{r}_l \cdot \mathbf{v}_l = 0$.

Finally, the mathematical model is concluded with the boundary conditions of torque and force free filament ends, which at $l = \pm L/2$ require

$$\mathbf{r}_l|_{l=\pm L/2} = \mathbf{0} \quad (5)$$

and

$$(-A_B \mathbf{r}_{lll} + \Lambda \mathbf{r}_l - \mu_0 M \mathbf{H})|_{l=\pm L/2} = \mathbf{0}. \quad (6)$$

¹We have corrected the final step of the calculation, where L in formula 3.93⁴ $L^{-4}A_B/\zeta$ needs to be taken as *half* of the filament's length.

2.1 Dimensionless parameters

The mathematical model can be rendered dimensionless by introducing the following scales:

- length scale $r_0 = L$,
- time scale $t_0 = \zeta_{\perp} L^4 / A_B$.

With this scaling, dimensionless parameters appear in the mathematical formulation:

- the magnetoelastic number $Cm = \mu_0 M H L^2 / A_B$,
- the ratio of perpendicular and parallel drag coefficients $\zeta_{\perp} / \zeta_{\parallel}$.

The ratio of drag coefficients is close to 2 for slender filaments [21]. If there is a rotating magnetic field driving the filament, a third dimensionless parameter arises:

- the Mason number $M_a = \omega \zeta_{\perp} L^2 / (12 \mu_0 M H)$,

where ω is the angular frequency of the field. The equations rendered dimensionless by r_0 and t_0 are used in section 3, where the equilibrium shape for small deformations is derived. Elsewhere to facilitate the reading, dimensional formulas are used.

3 Derivation of the equilibrium shape of a filament in a rotating field

To find the equilibrium shape of the filament in a rotating magnetic field, we can utilize the lack of inertia in the Stokes flow regime, and move to a coordinate system that rotates with the magnetic field (figure 1). We set the magnetic field along the x axis. A background flow of $\mathbf{v}_{\infty} = \{-\omega y, \omega x, 0\}$ arises, where ω is the angular velocity of the magnetic field. When $\omega = 0$, the filament lies along the x axis. We seek an approximate equilibrium shape up to first order in ω and y . The arclength parameter becomes $l = x + O(y^2)$.

With this approximation, along the x axis the equations stated in the section 2 read

$$\Lambda_x = 0, \tag{7}$$

where the subscript x denotes the derivative with respect to x . This together with the only non-trivial boundary condition

$$(-Cm + \Lambda)|_{x=\pm 1/2} = 0 \tag{8}$$

gives us the solution for the tension force

$$\Lambda = Cm. \tag{9}$$

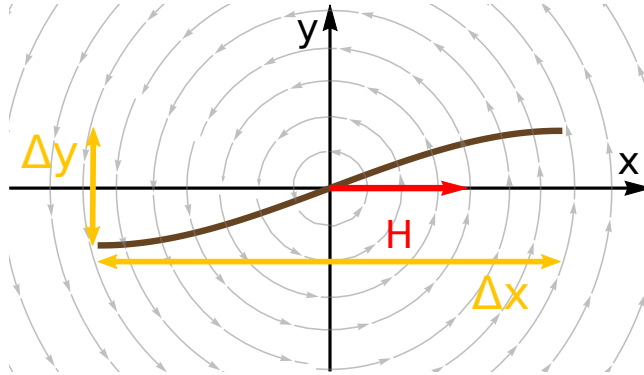


Figure 1: Sketch of the magnetic filament equilibrium shape in the reference frame of the rotating magnetic field. Δx and Δy show the difference of coordinates between the tips of the filament. The field is rotating clockwise, therefore in this reference frame there is a background flow counter-clockwise.

Along the y axis the equations stated in the section 2 read

$$-y_{xxxx} + \Lambda y_{xx} + \omega x = 0. \quad (10)$$

The boundary conditions are

$$y_{xx}|_{x=\pm 1/2} = 0, \quad (11)$$

$$(-y_{xxx} + \Lambda y_x)|_{x=\pm 1/2} = 0. \quad (12)$$

Plugging in Λ from equation (9), and requiring that $y(0) = 0$, we get the solution for the equilibrium shape of the filament

$$y = \frac{\omega}{12Cm} \left[\frac{6 \sinh(x\sqrt{Cm})}{Cm \sinh(\sqrt{Cm}/2)} - 2x^3 + x \left(\frac{3}{2} - \frac{12}{Cm} \right) \right]. \quad (13)$$

It is possible to verify that up to the first order in y , the filament inextensibility condition (eq. (4)) is satisfied. Additionally from the equation (13) it is evident that y is small when $\omega/(12Cm)$ is small, which suggests that $\omega/(12Cm) \ll 1$ is the criterion for the validity of this solution. The square-bracketed expression is bounded between $\pm 1/2$ for $x \in [-1/2, 1/2]$.

4 Analysis of the asymptotic equilibrium shape

For convenience from now on we will again use dimensional expressions. Equation (13) for the equilibrium shape in dimensional form reads

$$\frac{y}{L} = M_a \left[\frac{6 \sinh(x\sqrt{Cm}/L)}{Cm \sinh(\sqrt{Cm}/2)} - 2\frac{x^3}{L^3} + \frac{x}{L} \left(\frac{3}{2} - \frac{12}{Cm} \right) \right], \quad (14)$$

where we identify the coefficient in front of the brackets as the Mason number $M_a = \omega\zeta_{\perp}L^2/(12\mu_0MH)$, which is the ratio of viscous to magnetic forces in the system.

Interestingly, the tip coordinates of the filament are independent of Cm and are determined solely by M_a . Denoting with Δx and Δy the difference of x and y coordinates between the tips (figure 1), we can write

$$\frac{\Delta y}{\Delta x} = M_a. \quad (15)$$

This means that the expression in the square brackets solely determines the shape of the filament connecting the two end points. We plot the equation (14) divided with M_a for different values of Cm (see figure 2) to observe how this happens. For small values of Cm , the filament is nearly straight (which is expected, since in the limit of $A_B \rightarrow \infty$, the filament should be a rigid rod). Whereas large Cm means that the tips of the filament become bent in the direction of the field.

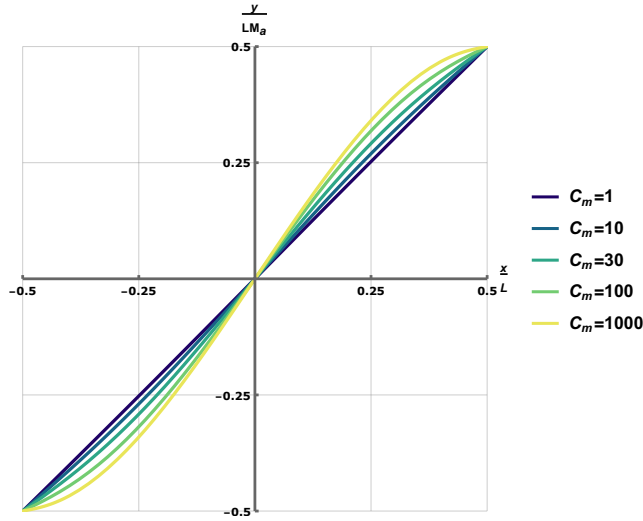


Figure 2: Illustration of how the magnetoelastic number Cm governs the shape of the filament according to eq. (14).

5 Correction to the asymptotic solution to take into account the limit of a rigid rotating rod

It is possible to write the equation for the deviation of a rigid ferromagnetic rod from the magnetic field direction [22]

$$\sin \theta = \frac{\Delta y}{L} = M_a, \quad (16)$$

where θ is the angle between the rod and the field, Δy and L are defined the same way as for the flexible filament. In terms of $y(l)$ the equation for the rigid rod ($Cm \rightarrow 0$) reads

$$y = M_a l. \quad (17)$$

Note that unlike eq. (14), eq. (17) is valid for arbitrary deviations from the magnetic field direction.

Knowing this, we can modify eq. (14) to include the limit of rigid rod as $Cm \rightarrow 0$. We write

$$\frac{y}{L} = M_a \left[\frac{6 \sinh(l\sqrt{Cm}/L)}{Cm \sinh(\sqrt{Cm}/2)} - 2 \frac{l^3}{L^3} + \frac{l}{L} \left(\frac{3}{2} - \frac{12}{Cm} \right) \right], \quad (18)$$

where we replaced $x \rightarrow l$. For small y/L , this corrected expression is asymptotically identical to the previously derived eq. (14). Whereas in the limit of small Cm , it is identical to the rigid rod (eq. (17)) for arbitrary y/L . Note that the formula only gives the y coordinate of the filament, however, the x coordinate can be determined by integrating $dx/dy = \sqrt{(dl/dy)^2 - 1}$.

We hope that this correction will improve the applicability range of the solution. Indeed looking at figure 3 we see that for small M_a and deviations from the magnetic field direction, the both eqs. (14) and (18) well coincide with the full numerical solution. As M_a increases the corrected eq. (18) follows the numerical shape much more closely, however, even it starts to noticeably deviate for $M_a > 0.5$. This is of course expected since in the derivation only the perpendicular drag coefficient ζ_{\perp} is used, but for larger deformations of the shape, the parallel drag coefficient ζ_{\parallel} starts to play a role.

6 Procedure to determine the filament parameters

The decoupling of the M_a and Cm effect on the shape (one determines the deviation from the field, while the other determines the shape) inspires us to propose the following procedure to determine them for an experimental filament.

1. Find the tips of the filament, and using eq. (16), determine the Mason number $M_a = \Delta y/L$.
2. Plug the found M_a in eq. (18) and determine Cm by varying it until it best describes the filament's shape.
3. Once the magnetic moment per unit length M is known, calculate the bending modulus $A_B = \mu_0 H M L^2 / Cm$.

Using this procedure, we determined the magnetoelastic Cm and Mason M_a numbers from the numerical equilibrium shapes. The relative error (*fitted* - *true*)/*true* of the parameters is shown in figure 4.

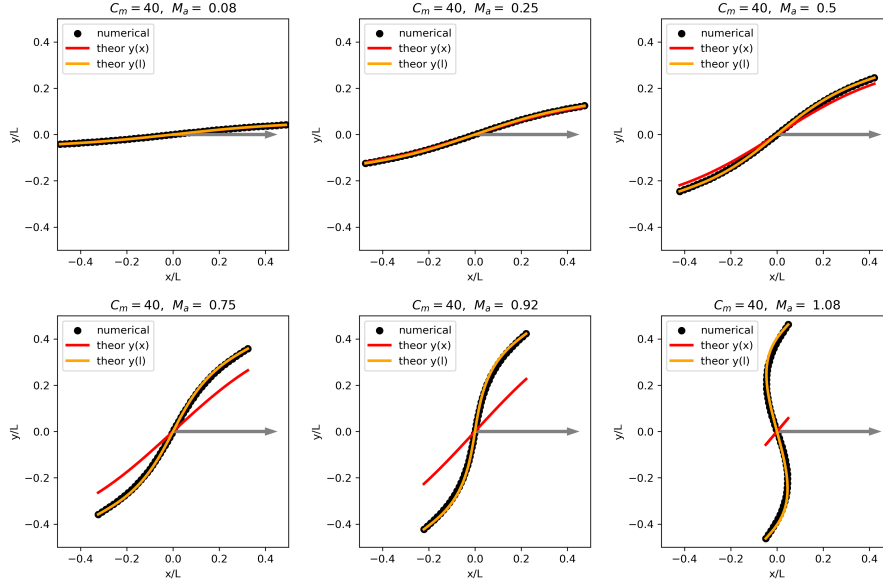


Figure 3: Equilibrium shapes of a rotating ferromagnetic filament for $Cm = 40$ and for different Ma . The drag coefficient ratio is $\zeta_{\perp}/\zeta_{\parallel} = 2$ in the numerical solution. The black dots show the numerical solution of the full problem, the red line shows the asymptotic solution (eq. (14)) valid for small Ma , the yellow line shows the corrected asymptotic solution (eq. (18)). The gray arrow shows the magnetic field direction.

The determined Ma is accurate for relatively large deviations from the magnetic field direction. The error in Ma is less than 10% for deviations of up to $\Delta y/L \approx 0.5$ from the magnetic field direction (which corresponds to roughly 30° between the filament and the field). The deviation from the magnetic field direction can be experimentally controlled by the rotation frequency. One should choose a low enough frequency such that the deviations are small, but the shape is still visually discernible. As expected, the equation (16) gives very accurate Ma values for small Cm , which corresponds to nearly rigid rod. However, increasing Cm values leads to an underestimate in Ma .

The error in the estimated Cm is noticeably larger, and is dependent on Cm itself. The method is most accurate for $Cm \approx 38$. As can be seen in figure 2, this is because for this Cm , the shape lies in between the two extreme configurations. To minimize the error one should find the magnetic field value such that the experimentally observed shape is between the extremes of a straight rod and an S shape, whose tips align with the magnetic field. Additionally, the deviation from the magnetic field direction should be less than $\approx 20^\circ$ and $Cm \approx 10 \dots 70$ to have the relative error of 15...20%. Interestingly, the error seems to be systematic - the method underestimates the true Cm value. We can therefore increase the

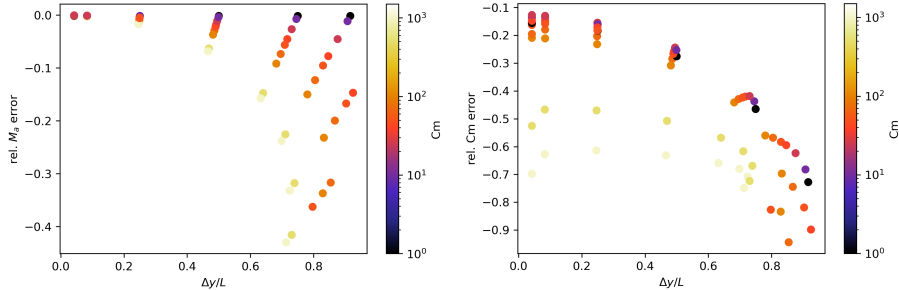


Figure 4: The relative error of the fitted M_a (left) and Cm (right) as a function of the tip deviation from the magnetic field direction $\Delta y/L$. The value of the magnetoelastic number Cm used in the numerical equilibrium shapes is given by the color.

fitted Cm by $\approx 15\%$ to get a more accurate result.

To conclude the section let us examine a particular experimental observation (figure 1 (a) in ref. [15], whose data are archived in ref. [23]). We used the procedure outlined in the beginning of this section to estimate the M_a and Cm numbers. Experimental filament's shape is taken from the center coordinates of the beads that make up the filament. From the centers of the first and last bead of the filament we get $M_a = 0.31$, and the shape fit then gives us $Cm = 40 \pm 15$, which we can increase by $\approx 15\%$ (to offset the systematic underestimate as seen in figure 4) to obtain $Cm = 46$. From magnetization measurements it was found that these beads possess a magnetic moment of $m = 1.4 \cdot 10^{-13} A \cdot m^2$ [5]. Dividing by their typical diameter $d = 4.26 \mu m$ gives us the linear magnetization of the filament $M = 3.3 \cdot 10^{-8} A \cdot m$. The length of the filament in the experiment is $L = 67.4 \mu m$, and the magnetic field is $\mu_0 H = 0.86 mT$. This allows us to determine the bending modulus $A_B = \mu_0 H M L^2 / Cm = 2.8 \cdot 10^{-21} J \cdot m$. This result falls in the middle of the values shown in table 1. Finally, for comparison the effective bending elasticity that arises just from the interaction between magnetic dipoles in the chain is two orders of magnitude smaller $A_B^{mag} = \mu_0 M^2 (\zeta(3) + 1/6) / (18\pi) = 3.3 \cdot 10^{-23} J \cdot m$ [24], where $\zeta(n)$ is the Riemann zeta function. This confirms that the bending stiffness mostly comes from the DNA linkers between the beads.

7 Conclusions

The equilibrium shape of a ferromagnetic filament in a rotating field contains the information about the filament's properties. In particular, the tip positions relative to the magnetic field direction encode the value of the Mason number M_a - the ratio of magnetic to viscous forces. The shape that connects the tips is only dependent on the magnetoelastic number Cm - the ratio of magnetic to elastic forces. For small values of Cm the filament takes up a straight shape

like a rigid magnetic rod, while for a large Cm the filament's tips bend in the direction of the magnetic field, resulting in an S-like shape. This allows us to determine Cm just by visually observing the shape of the filament. Once we know the magnetization of the filament, we can also determine the bending modulus A_B .

Declaration of Competing Interest

The authors declare that they have no known competing financial interests or personal relationships that could have appeared to influence the work reported in this paper.

Acknowledgements

Authors acknowledge the funding by the Latvian Council of Science, project A4Mswim, project No. lzp-2021/1-0470.

References

- [1] C. Goubault, P. Jop, M. Fermigier, J. Baudry, E. Bertrand, and J. Bibette, "Flexible Magnetic Filaments as Micromechanical Sensors," *Physical Review Letters*, vol. 91, no. 26, p. 260 802, 2003. DOI: 10.1103/PhysRevLett.91.260802.
- [2] S. L. Biswal and A. P. Gast, "Rotational dynamics of semiflexible paramagnetic particle chains," *Physical Review E*, vol. 69, no. 4, p. 041 406, 2004. DOI: 10.1103/PhysRevE.69.041406.
- [3] T. Yang, D. W. Marr, and N. Wu, "Superparamagnetic colloidal chains prepared via Michael-addition," *Colloids and Surfaces A: Physicochemical and Engineering Aspects*, vol. 540, pp. 23–28, 2018. DOI: 10.1016/j.colsurfa.2017.12.044.
- [4] A. Spatafora-Salazar, D. M. Lobmeyer, L. H. P. Cunha, K. Joshi, and S. L. Biswal, "Hierarchical assemblies of superparamagnetic colloids in time-varying magnetic fields," *Soft Matter*, vol. 17, no. 5, pp. 1120–1155, 2021. DOI: 10.1039/D0SM01878C.
- [5] K. Erglis, R. Livanovičs, and A. Cēbers, "Three dimensional instability of the flexible ferromagnetic filament loop," *Magnetohydrodynamics*, vol. 46, no. 3, pp. 245–256, 2010. DOI: 10.22364/mhd.46.3.2.
- [6] J. Byrom, P. Han, M. Savory, and S. L. Biswal, "Directing Assembly of DNA-Coated Colloids with Magnetic Fields To Generate Rigid, Semiflexible, and Flexible Chains," *Langmuir*, vol. 30, no. 30, pp. 9045–9052, 2014. DOI: 10.1021/1a5009939.

- [7] R. Dreyfus, J. Baudry, M. L. Roper, M. Fermigier, H. A. Stone, and J. Bibette, “Microscopic artificial swimmers,” *Nature*, vol. 437, no. 7060, pp. 862–865, 2005. DOI: 10.1038/nature04090.
- [8] A. Zaben, G. Kitenbergs, and A. Cēbers, “Instability caused swimming of ferromagnetic filaments in pulsed field,” *Scientific Reports*, vol. 11, no. 1, p. 23 399, 2021. DOI: 10.1038/s41598-021-02541-3.
- [9] S. L. Biswal and A. P. Gast, “Micromixing with Linked Chains of Paramagnetic Particles,” *Analytical Chemistry*, vol. 76, no. 21, pp. 6448–6455, 2004. DOI: 10.1021/ac0494580.
- [10] R. Zhang, J. D. Toonder, and P. R. Onck, “Metachronal patterns by magnetically-programmable artificial cilia surfaces for low Reynolds number fluid transport and mixing,” *Soft Matter*, vol. 18, no. 20, pp. 3902–3909, 2022. DOI: 10.1039/D1SM01680F.
- [11] T. Yang *et al.*, “Reconfigurable microbots folded from simple colloidal chains,” *Proceedings of the National Academy of Sciences*, vol. 117, no. 31, pp. 18 186–18 193, 2020. DOI: 10.1073/pnas.2007255117.
- [12] A. Cebers and K. Erglis, “Flexible Magnetic Filaments and their Applications,” *Advanced Functional Materials*, vol. 26, no. 22, pp. 3783–3795, 2016. DOI: 10.1002/adfm.201502696.
- [13] M. Belovs and A. Cēbers, “Equilibrium shapes and stability of magnetic filaments,” *Physical Review E*, vol. 105, no. 1, p. 014 601, 2022. DOI: 10.1103/PhysRevE.105.014601.
- [14] C. H. Wiggins, D. Rivelino, A. Ott, and R. E. Goldstein, “Trapping and Wiggling: Elastohydrodynamics of Driven Microfilaments,” *Biophysical Journal*, vol. 74, no. 2, pp. 1043–1060, 1998. DOI: 10.1016/S0006-3495(98)74029-9.
- [15] A. Zaben, G. Kitenbergs, and A. Cēbers, “Deformation of flexible ferromagnetic filaments under a rotating magnetic field,” *Journal of Magnetism and Magnetic Materials*, vol. 499, p. 166 233, 2020. DOI: 10.1016/j.jmmm.2019.166233.
- [16] L. Koens and T. D. Montenegro-Johnson, “Local drag of a slender rod parallel to a plane wall in a viscous fluid,” *Physical Review Fluids*, vol. 6, no. 6, p. 064 101, 2021. DOI: 10.1103/PhysRevFluids.6.064101.
- [17] K. Ērglis, M. Belovs, and A. Cēbers, “Flexible ferromagnetic filaments and the interface with biology,” *Journal of Magnetism and Magnetic Materials*, vol. 321, no. 7, pp. 650–654, 2009. DOI: 10.1016/j.jmmm.2008.11.047.
- [18] A. Zaben, G. Kitenbergs, and A. Cēbers, “3D motion of flexible ferromagnetic filaments under a rotating magnetic field,” *Soft Matter*, vol. 16, no. 18, pp. 4477–4483, 2020. DOI: 10.1039/D0SM00403K.
- [19] K. Ērglis, “Experimental study of properties and motion of flexible magnetic microfilaments,” PhD, University of Latvia, 2010. [Online]. Available: <https://dspace.lu.lv/dspace/handle/7/5160>.

- [20] A. Cebers, “Dynamics of a chain of magnetic particles connected with elastic linkers,” *Journal of Physics: Condensed Matter*, vol. 15, no. 15, S1335–S1344, 2003. DOI: 10.1088/0953-8984/15/15/303.
- [21] E. Lauga, *The Fluid Dynamics of Cell Motility*, 1st ed. Cambridge University Press, 2020. DOI: 10.1017/9781316796047.
- [22] L. Goyeau, R. Livanovičs, and A. Cēbers, “Dynamics of a flexible ferromagnetic filament in a rotating magnetic field,” *Physical Review E*, vol. 96, no. 6, p. 062612, 2017. DOI: 10.1103/PhysRevE.96.062612.
- [23] A. Zaben, G. Kitenbergs, and A. Cebers, *Data for the article “Deformation of flexible ferromagnetic filaments under a rotating magnetic field”*, 2020. DOI: 10.5281/ZENODO.3701572.
- [24] D. Vella, E. Du Pontavice, C. L. Hall, and A. Goriely, “The *magneto-elastica* : From self-buckling to self-assembly,” *Proceedings of the Royal Society A: Mathematical, Physical and Engineering Sciences*, vol. 470, no. 2162, p. 20130609, 2014. DOI: 10.1098/rspa.2013.0609.